Organometallic Complexes of Uracil and Orotic Acid Derivatives: Coordination Mode, Structure, and Reactivity

Donald J. Darensbourg,*[a] Brian J. Frost,[a] David L. Larkins,[a] and Joseph H. Reibenspies[a]

Keywords: Carbonyl complexes / Uracil / Pyrimidines / Kinetics

Carbonyltungsten derivatives of uracilates and orotates, where the metal center is bound to a nitrogen atom of the pyrimidine ring, are described. There organometallic complexes were synthesized by the reaction of either $W(CO)_5THF$ or $W(CO)_5MeOH$ with the tetraethylammonium salt of the deprotonated monoanion of dihydrouracil (**1**), 5-methyluracil (**2**), 6-methyluracil (**3**), methylorotic acid (**4**), and *N*,*N*-dimethylorotic acid (**5**). The complexes were all characterized in solution by IR and ^{13}C NMR spectroscopy, and in select instances in the solid-state by X-ray crystallography. The structures of complexes **1** and **3** consist of octahedrally coordinated anions of pentacarbonyltungsten uracilate, where the uracilate ligand is bound to the metal center by the N3 atom of the pyrimidine ring, and the tetraethylammonium cation for charge balance. In contrast, the anion of complex **2** reveals that the uracilate ligand is bound to the $W(CO)_5$ fragment by the N1 atom of the pyrimidine ring. The ν(CO) vibrational modes and ^{13}C NMR chemical shifts for the carbonyl ligands of complexes **1** and **3** indicate that the metal centers are more electron-rich than those of complex **2**. This conclusion is further substantiated by the rates of intermolecular CO exchange in these carbonylmetal anions with ^{13}CO. The facile CO exchange observed in complexes **1** and **3** is faster than that seen in complex **2**. The rapid CO dissociation process measured in these derivatives is attributed to the π-donation of electron density from the pyrimidine ring to the tungsten center in the transition state as the M–CO bond is broken.

Introduction

The coordination chemistry of pyrimidine bases has been a subject of interest for many years, and has been studied from a variety of perspectives by many different research groups.[1−4] Pyrimidine derivatives of thymine and uracil, such as AZT (3′-azido-3′-deoxythymidine), have been shown to be effective antiviral drugs.[5,6] Metal complexes of pyrimidines have been shown to be useful as biological carriers for some of these drugs such as AZT,[7−10] others have demonstrated anti-cancer/tumor activity.[11,12] Despite the plethora of coordination complexes of pyrimidines, the organometallic chemistry involving these ligands has received limited attention, with most efforts coming from the laboratory of Beck and co-workers.[13,14] Recently, we have examined the coordination modes of uracils and orotic acid derivatives to zero-valent group-6 carbonylmetal compounds, focusing our studies on the ability of the ring nitrogen atoms to serve as π-donor ligands and to facilitate CO dissociation.[15,16] Previously, investigations of the coordination chemistry of uracils have revealed a wide range of metal-dependent binding modes, including via N1, N3, the exocyclic oxygen atoms,[1,2] both an endocyclic nitrogen and an exocyclic oxygen (or sulfur) atom,[15,17] and finally, though less common, through C5.[18]

Herein, we wish to communicate a continuation of our studies of organometallic derivatives of uracils and orotic acid derivatives. Specifically, this study will examine the various coordination modes and π-donor abilities of a series of tungsten-bound uracilate and orotate derivatives, in particular dihydrouracil, 5-methyluracil (thymine), 6-methyluracil, methylorotic acid, and *N*,*N*-dimethylorotic acid (Scheme 1). Also discussed are the electronic effects of different pyrimidine derivatives as examined by IR and ^{13}C NMR spectroscopy, and CO exchange kinetics.

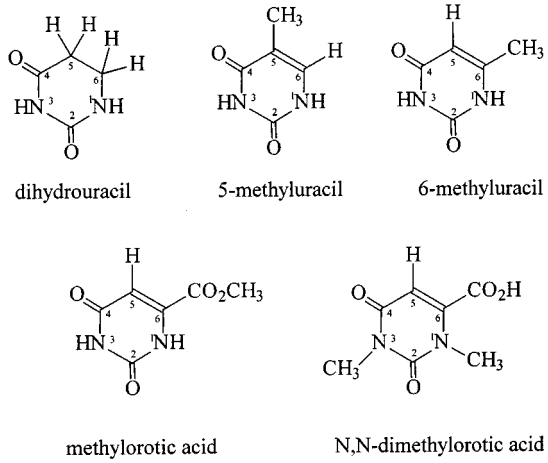

Scheme 1

Results and Discussion

A series of $[Et_4N][W(CO)_5L]$ complexes, where L = dihydrouracilate (**1**), 5-methyluracilate (**2**), 6-methyluracilate (**3**), methylorotate (**4**), and *N*,*N*-dimethylorotate (**5**), were synthesized in good yields by the labile-ligand displacement of THF or methanol from $W(CO)_5(THF)$ or $W(CO)_5(MeOH)$

[a] Texas A&M University, Department of Chemistry, College Station, Texas 77843, USA

  1434−1948/00/1212−2487 $ 17.50+.50/0

Table 1. Stretching frequencies of the carbonyl ligands in complexes **1**−**5**, and other related complexes

Complex[a][b]	ν(CO) [cm^{-1}]			ν(CO_2) [cm^{-1}]	
$[W(CO)_5$(dihydrouracilate)]$^-$ (**1**)	2057.9 (w)	1910.4 (vs)	1839.0 (m)	1660.6	1597.9
$[W(CO)_5$(5-methyluracilate)]$^-$ (**2**)	2064.7 (w)	1915.2 (vs)	1855.4 (m)	1660.6	1637.5
$[W(CO)_5$(6-methyluracilate)]$^-$ (**3**)	2058.9 (w)	1912.3 (vs)	1840.0 (m)	1663.5	1571.9
$[W(CO)_5$(methylorotate)]$^-$ (**4**)	2059.9 (w)	1914.2 (vs)	1845.8 (m)	1665.4	1644.2
$[W(CO)_5$(*N*,*N*-dimethylorotate)]$^-$ (**5**)	2067.6 (w)	1920.9 (vs)	1853.5 (m)	1661.5	1647.1
$[W(CO)_5$(uracilate)]$^-$	2065.6 (w)	1917.1 (vs)	1858.3 (m)	1668.3	1637.5[c]

[a] As the tetraethylammonium salt. − [b] Spectra determined in CH_3CN. − [c] Ref.[15]

[prepared in situ by photolysis of $W(CO)_6$ in THF or meth-1anol] by the tetraethylammonium salt of the deprotonated monoanion of the corresponding uracil or orotic acid derivative. All complexes were characterized by IR and ^{13}C NMR spectroscopy in the carbonyl region, elemental analysis, and X-ray crystallography for complexes **1**−**3**. In addition, the product of the reaction of **1** with methanol, $[Et_4N]_2[W_2(CO)_8(OMe)_2]$ (**6**), was also characterized by X-ray crystallographic analysis and ^{13}C NMR spectroscopy.

The IR spectra in the ν(CO) stretching region of complexes **1**−**5** consist of three bands of the appropriate intensity pattern for a $W(CO)_5$ fragment of C_{4v} local symmetry. Table 1 contains the ν(CO) values for these, and closely related, derivatives. Since the ν(CO) stretching vibrational modes are such good probes of the electron-donating ability of the ancillary ligands bound to the metal center in the carbonylmetal derivatives, it is clear from a close scrutiny of the ν(CO) spectra of complexes **2** and **3** (Figure 1) that the uracilate ligands are coordinated differently in these instances. That is, there is a significant difference in the low-frequency A_1 modes of these two derivatives, where the electronic effects of the uracilate-binding mode should be most evident. Similarly, the pyrimidine carbonyl stretches are also quite different, with the $\Delta\nu(CO_2)$ for the asymmetric and symmetric vibrations being 23 and 92 cm^{-1} for **2** and **3**, respectively. Furthermore, based on the similarity of the ν(CO) spectra of complexes **1**, **3**, and **4**, it is reasonable to suggest that in these derivatives the pyrimidine ligands are bonded in a similar fashion. It is also evident from the ν(CO) IR data listed in Table 1 that complex **2** and the structurally characterized $[Et_4N][W(CO)_5$(uracilate)] derivative[15] share a common structure. The *N*,*N*′-dimethylorat-

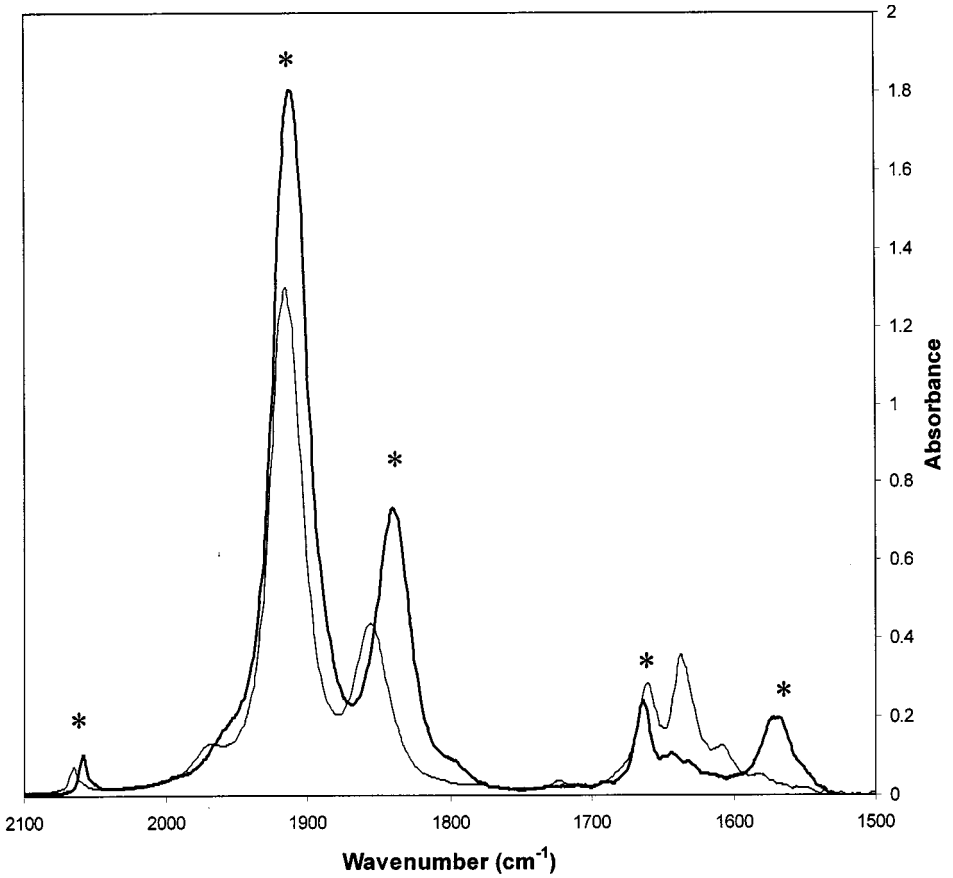

Figure 1. Infrared spectra in the ν(CO) and ν(CO_2) regions of $[Et_4N][W(CO)_5$(5-methyluracilate)] (**2**) and $[Et_4N][W(CO)_5$(6-methyluracilate) (**3**) in acetonitrile solvent; peaks marked with asterisks are those due to complex **3**

ate derivative, complex **5**, exhibits ν(CO) IR bands typical of carboxylates bound in a monodentate fashion containing electron-withdrawing substituents in anionic complexes of the type $W(CO)_5$(carboxylate)$^-$. For example, the $W(CO)_5(O_2CCF_3)^-$ anion has ν(CO) vibrational modes at 2066, 1916, and 1857 cm^{-1} in THF solution.[19]

^{13}C NMR spectroscopic data for the carbonyl ligands were compiled for complexes **1**−**6**, and are listed in Table 2. Complexes **1**−**5** exhibit the anticipated two ^{13}C resonances of intensity ratio 1:4, with the more intense upfield signal corresponding to that of the four *cis* carbonyl ligands. Complex **2** displays ^{13}C NMR signals for the equatorial and axial CO ligands at δ = 200.6 and 205.7, respectively, which are quite similar to values previously reported for the carbonyl ligands of the $W(CO)_5$(uracilate)$^-$ anion.[15] On the other hand, complexes **1**, **3**, and **4** exhibit ^{13}C NMR resonances which are measurably different from complex **2** and $[Et_4N][W(CO)_5$(uracilate)], again suggesting a different coordination mode for these latter two pyrimidine derivatives.

Table 2. ^{13}C NMR data for the carbonyl ligands in complexes **1**−**6**

Complex[a]	^{13}C resonance, δppm ($^1J_{W-C}$ [Hz]) CO (equatorial)	CO (axial)
$[W(CO)_5$(dihydrouracilate)]$^-$ (**1**)	203.0 (130)	208.5 (149)[b]
$[W(CO)_5$(5-methyluracilate)]$^-$ (**2**)	200.7 (131)	205.8[c]
$[W(CO)_5$(6-methyluracilate)]$^-$ (**3**)	202.0 (131)	204.8[c]
$[W(CO)_5$(methylorotate)]$^-$ (4)	201.7 (131)	207.9[c]
$[W(CO)_5$(*N*,*N*-dimethylorotate)]$^-$ (**5**)	200.7	205.8[c]
$[W_2(CO)_8(OMe)_2]^{2-}$ (**6**)	208.5	220.1[d]
$[W_2(CO)_6(OMe)_3]^{3-}$	234.1[d]	

[a] As the tetraethylammonium salt. − [b] Spectrum determined in THF/CD_3CN. − [c] Spectrum determined in CD_3CN. − [d] Spectrum determined in [D_4]methanol.

In order to address the question of the coordination modes of the pyrimidines definitively, the structures of complexes **1**−**3** were determined in the solid state by X-ray crystallography. The structures of all three derivatives are quite similar with five of the octahedral coordination sites occupied by carbonyl ligands and the sixth position occupied by a pseudo-amido donor from the pyrimidine base. Indeed, the differences in these structures lie in the pyrimidine ring/coordination mode. That is, in complexes **1** and **3** the pyrimidine ligand is bound through the deprotonated N3 nitrogen atom of the pyrimidine ring. In contrast, complex **2** contains a pyrimidine ring bound to the tungsten center through the deprotonated N1 nitrogen atom in a manner analogous to that previously reported for the $W(CO)_5$(uracilate)$^-$ anion.[15] Coordination through the N3 nitrogen atom of the pyrimidine ring places the exocyclic oxygen atoms in close proximity to the metal center, thereby assisting in the loss of a CO ligand with concomitant formation of a tetracarbonyl derivative containing a chelating uracilate ligand. For example, the tetracarbonyl derivative of complex **3** has been characterized by ν(CO) IR: 1991(w), 1865(s), 1840(m), and 1808(m) in THF; and by ^{13}C NMR: δ = 208.1 (2 *C*O), 217.7 (1 *C*O), and 218.3 (1 *C*O) in CD_3CN.

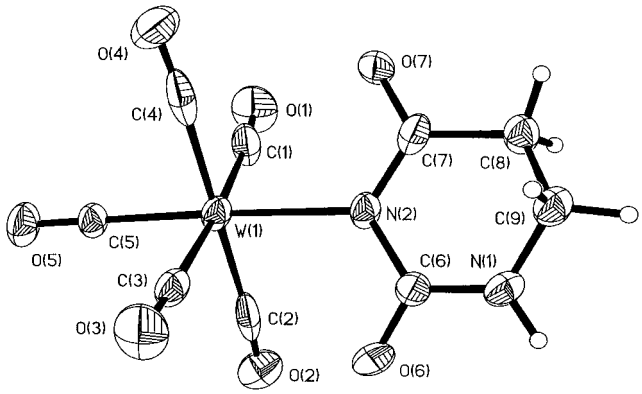

Figure 2. Thermal ellipsoid representation of the anion of complex **1**, $W(CO)_5$(dihydrouracilate)$^-$

Crystals of complex **1** suitable for X-ray analysis were obtained by the slow diffusion of hexane into a THF solution of the complex maintained at 0 °C. A thermal ellipsoid drawing of the monoanion, $W(CO)_5$(dihydrouracilate)$^-$, is depicted in Figure 2 along with the atomic numbering scheme. Selected bond lengths and bond angles are listed in Table 3. The crystal lattice of complex **1** contains a tetraethylammonium cation (for charge balance), as well as a diethyl ether molecule of solvation. The octahedral environment about the tungsten center consists of a dihydrouracilate anion bound to the metal center through the N3 atom of the pyrimidine ring at a distance of 2.263(8) Å. This bond length compares well with other related W−N bond lengths which are summarized in Table 4.[20−22] The *trans*-CO ligand exhibits a slightly shorter W−C bond length [1.967(10) Å] than the average W−C distance for the four *cis*-CO ligands [2.061(16) Å]. As anticipated, the pyrimidine ring in complex **1** is non-planar (Figure 3), unlike those in complexes **2** and **3** (vide supra) where the ring is pseudoaromatic.

The solid-state structure of complexes **2** and **3** were determined by crystallographic analysis on crystals obtained from the slow diffusion of hexane into a THF solution of the respective complex at ambient temperature. Thermal ellipsoid drawings of the anions of complexes **2** and **3** are shown in Figure 4 and Figure 5, respectively. Table 5 and Table 6 compile selected bond lengths and bond angles for these derivatives.

In complex **2**, the pyrimidine ligand is bound through the deprotonated N1 position of the ring like that observed in the parent $W(CO)_5$(uracilate)$^-$ anion.[15] On the other hand, the [$W(CO)_5$] fragment in complex **3** is bound through the deprotonated N3 position of the pyrimidine ring, much like that seen in complex **1**. The choice of binding modes appears to be mainly a consequence of steric interactions. As is apparent from the space-filling models for the anions of complexes **2** and **3** (Figure 6), the methyl substituent on the pyrimidine ring precludes binding at the N1 site in complex **3**.

On the other hand, for all other structures we have determined herein and elsewhere,[15] binding occurs at the N1

Table 3. Selected bond lengths [Å] and angles [°] for **1**; estimated standard deviations are given in parentheses

W1−C5	1.967(10)	W1−C4	2.07(2)
W1−C1	2.045(12)	W1−C2	2.07(2)
W1−C3	2.059(12)	W1−N2	2.263(8)
O1−C1	1.134(14)	N1−C9	1.447(14)
O5−C5	1.149(13)	C7−C8	1.513(14)
O2−C2	1.16(2)	C8−C9	1.512(14)
O3−C3	1.136(15)	N2−C7	1.365(14)
O4−C4	1.16(2)	N2−C6	1.413(13)
O7−C7	1.222(13)	N1−C6	1.334(14)
O6−C6	1.238(13)		
C5−W1−C1	88.0(4)	O1−C1−W1	174.6(10)
C5−W1−C3	88.8(4)	O5−C5−W1	179.7(12)
C1−W1−C3	175.9(4)	O2−C2−W1	175.6(10)
C5−W1−C4	90.2(4)	O3−C3−W1	177.3(10)
C1−W1−C4	85.9(5)	O4−C4−W1	175.1(10)
C3−W1−C4	91.7(5)	O7−C7−N2	121.1(9)
C5−W1−C2	88.6(4)	O7−C7−C8	119.5(10)
C1−W1−C2	90.9(5)	N2−C7−C8	119.2(9)
C3−W1−C2	91.5(5)	C9−C8−C7	112.5(9)
C4−W1−C2	176.6(4)	N1−C9−C8	107.5(9)
C5−W1−N2	177.1(3)	O6−C6−N1	120.1(9)
C1−W1−N2	94.7(4)	O6−C6−N2	119.2(9)
C3−W1−N2	88.5(4)	N1−C6−N2	120.7(9)
C4−W1−N2	90.9(4)	C7−N2−W1	120.8(6)
C2−W1−N2	90.4(4)	C6−N2−W1	120.4(6)
C7−N2−C6	118.9(8)	C6−N1−C9	123.1(9)

Table 4. W−N bond lengths for complexes **1−3**, as well as other similar complexes

Complex[a]	W−N [Å]	Ref.
$[W(CO)_5$(dihydrouracilate)$]^-$ (**1**)	2.263(8)	this work
$[W(CO)_5$(5-methyluracilate)$]^-$ (**2**)	2.236(15)	this work
$[W(CO)_5$(6-methyluracilate)$]^-$ (**3**)	2.276(4)	this work
$[W(CO)_5$(uracilate)$]^-$	2.281(8)	[15]
$[W(CO)_4$(orotate)$]^{2-}$	2.258(9)	[15]
$[W(CO)_4$(dihydroorotate)$]^{2-}$	2.231(13)	[15]
$[W(CO)_4$(glycinate)$]^-$	2.328(22)	[20]
$W(CO)_5$(piperidine)	2.331(5)	[21]
$W(CO)_5$(pyridine)	2.26(1)	[22]

[a] As the tetraethylammonium salt.

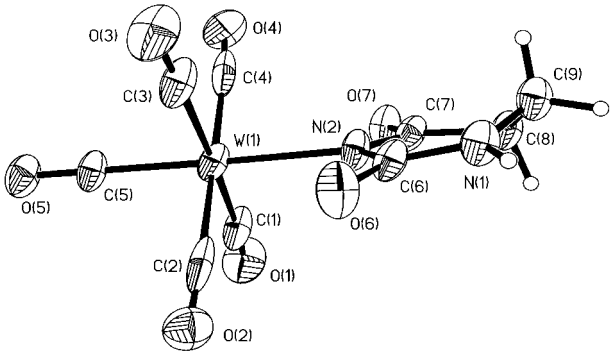

Figure 3. Thermal ellipsoid drawing of the anion of complex **1**, $W(CO)_5$(dihydrouracilate)$^-$, illustrating the puckering of the dihydrouracilate ring

site in the absence of steric hindrance. This is consistent as well with the prediction based on spectroscopic data that suggest complex **4** to be bound at the N3 site. In this instance the steric bulk of $-CO_2CH_3$ would inhibit binding at

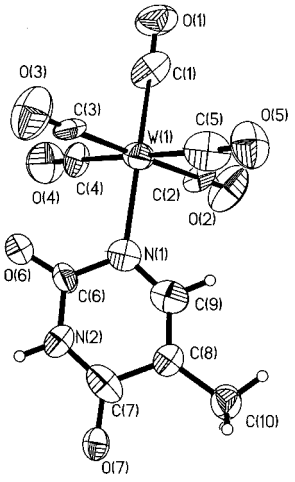

Figure 4. Thermal ellipsoid representation of the anion of complex **2**, $W(CO)_5$(5-methyluracilate)$^-$

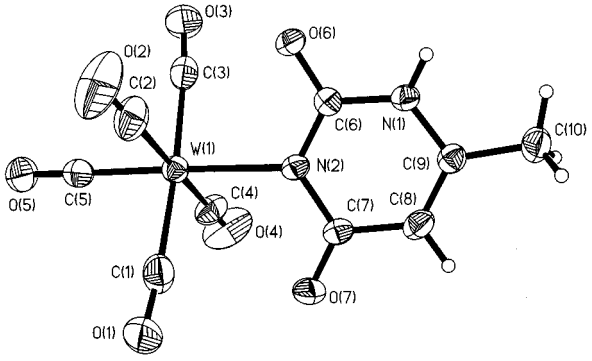

Figure 5. Thermal ellipsoid representation of the anion of complex **3**, $W(CO)_5$(6-methyluracilate)$^-$

Table 5. Selected bond lengths [Å] and angles [°] for **2**; estimated standard deviations are given in parentheses

W(1)−C(5)	1.98(2)	C(1)−O(1)	1.12(2)
W(1)−C(2)	2.006(19)	N(1)−C(9)	1.33(2)
W(1)−C(3)	2.05(2)	N(1)−C(6)	1.39(2)
W(1)−C(4)	2.07(2)	C(6)−O(6)	1.18(2)
W(1)−C(1)	2.05(3)	C(6)−N(2)	1.37(2)
W(1)−N(1)	2.236(15)	N(2)−C(7)	1.33(3)
C(5)−O(5)	1.14(2)	C(7)−O(7)	1.29(2)
C(2)−O(2)	1.11(2)	C(7)−C(8)	1.46(2)
C(4)−O(4)	1.15(2)	C(8)−C(9)	1.36(2)
C(3)−O(3)	1.11(2)	C(8)−C(10)	1.51(2)
C(1)−W(1)−C(2)	89.5(8)	O(3)−C(3)−W(1)	174.8(18)
C(1)−W(1)−C(4)	88.9(8)	O(4)−C(4)−W(1)	178(2)
C(2)−W(1)−C(4)	90.0(9)	O(5)−C(5)−W(1)	175.5(19)
C(1)−W(1)−C(3)	89.4(7)	C(9)−N(1)−C(6)	115.6(17)
C(2)−W(1)−C(3)	178.7(7)	C(9)−N(1)−W(1)	124.6(12)
C(4)−W(1)−C(3)	89.2(8)	C(6)−N(1)−W(1)	119.8(13)
C(1)−W(1)−C(5)	90.6(8)	O(6)−C(6)−N(2)	117.1(16)
C(2)−W(1)−C(5)	89.5(9)	O(6)−C(6)−N(1)	126.0(18)
C(4)−W(1)−C(5)	179.3(8)	N(2)−C(6)−N(1)	116.7(18)
C(3)−W(1)−C(5)	91.2(9)	C(7)−N(2)−C(6)	127.3(16)
C(1)−W(1)−N(1)	179.3(6)	O(7)−C(7)−N(2)	124.5(17)
C(2)−W(1)−N(1)	91.0(6)	O(7)−C(7)−C(8)	118(2)
C(4)−W(1)−N(1)	91.6(7)	N(2)−C(7)−C(8)	117.2(18)
C(3)−W(1)−N(1)	90.1(6)	C(9)−C(8)−C(7)	111.3(18)
C(5)−W(1)−N(1)	88.9(7)	C(9)−C(8)−C(10)	124.4(18)
O(1)−C(1)−W(1)	178.1(18)	C(7)−C(8)−C(10)	124.2(18)
O(2)−C(2)−W(1)	175.5(19)	N(1)−C(9)−C(8)	131.4(19)

Table 6. Selected bond lengths [Å] and angles [°] for **3**; estimated standard deviations are given in parentheses

W1−C5	1.952(5)	N1−C6	1.373(5)
W1−C2	2.028(6)	N2−C6	1.354(6)
W1−C3	2.039(6)	N2−C7	1.398(5)
W1−C4	2.045(6)	N1−C9	1.373(6)
W1−C1	2.046(6)	O6−C6	1.248(5)
W1−N2	2.276(4)	C10−C9	1.493(6)
O1−C1	1.144(7)	C7−O7	1.234(5)
O2−C2	1.151(8)	C7−C8	1.450(6)
O3−C3	1.148(7)	C8−C9	1.347(7)
O4−C4	1.137(7)	O5−C5	1.170(6)
C5−W1−C2	88.1(2)	C7−N2−W1	120.3(3)
C5−W1−C3	87.4(2)	C9−N1−C6	123.3(4)
C2−W1−C3	88.9(2)	O7−C7−N2	121.1(4)
C5−W1−C4	89.4(2)	O7−C7−C8	121.3(4)
C2−W1−C4	176.1(2)	N2−C7−C8	117.6(4)
C3−W1−C4	88.0(2)	C9−C8−C7	121.2(4)
C5−W1−C1	88.3(2)	C8−C9−N1	117.7(4)
C2−W1−C1	92.0(3)	C8−C9−C10	125.7(4)
C3−W1−C1	175.5(2)	N1−C9−C10	116.6(4)
C4−W1−C1	90.9(2)	O6−C6−N2	122.2(4)
C5−W1−N2	177.9(2)	O6−C6−N1	118.0(4)
C2−W1−N2	93.9(2)	N2−C6−N1	119.8(4)
C3−W1−N2	93.0(2)	O3−C3−W1	174.9(5)
C4−W1−N2	88.6(2)	O4−C4−W1	177.1(5)
C1−W1−N2	91.4(2)	O5−C5−W1	178.9(4)
O1−C1−W1	173.5(5)	C6−N2−C7	120.1(4)
O2−C2−W1	175.3(5)	C6−N2−W1	119.5(3)

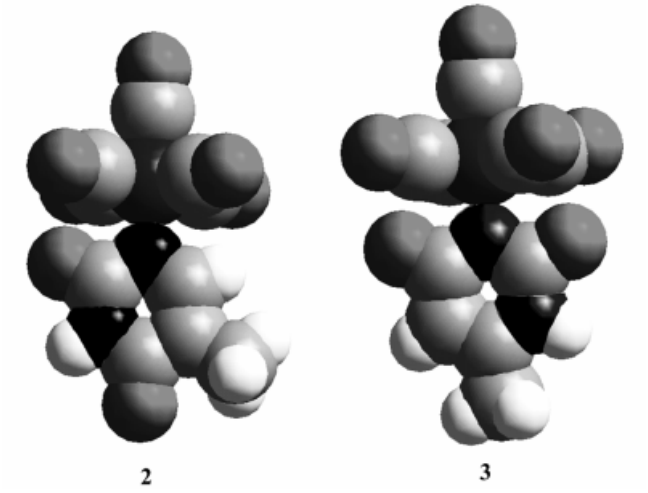

Figure 6. Space-filling models of the anions of complex **2** (left) and **3** (right)

N1. The tungsten−nitrogen distances are 2.236(15) Å and 2.276(4) Å, respectively, in complexes **2** and **3**. The W−C distances in the two derivatives are similar as expected, with both exhibiting a *trans* effect. That is, the W−C distance *trans* to the pyrimidine ligand is shorter than the average W−C distance *cis* to the pyrimidine ligand. For example, in complex **3**, the W−C *trans* distance is 1.952(5) Å, whereas the average W−C *cis* bond length is 2.040(6) Å. The packing diagrams of complexes **1**−**3** reveal that there is substantial amount of hydrogen bonding that is prevalent in the crystal structures of these complexes, as might be anticipated for pyrimidine derivatives. This is illustrated in Figure 7, which depicts the base-pairing observed in complex **3**, where the average O···N distance is 2.754 Å.

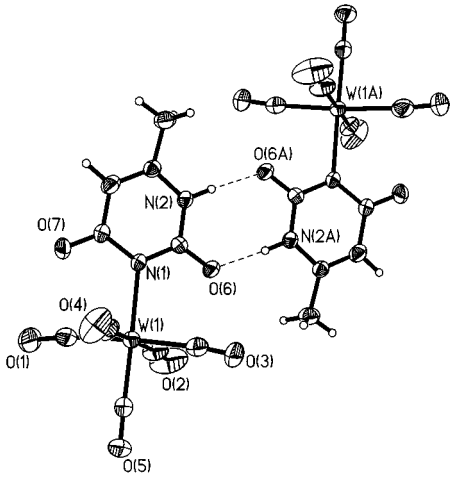

Figure 7. Thermal ellipsoid representation of the anions of complex **3**, $W(CO)_5$(6-methyluracilate)$^-$, showing the hydrogen-bonding motif between base pairs

These pyrimidine derivatives of carbonyltungsten are unstable in protic solvents. For example, on dissolving complex **1** in methanol the solution rapidly underwent a color change from orange to bright red and back to orange. Crystals of complex **6**, $[Et_4N]_2[W(CO)_4OMe]_2$ were isolated from a sample of **1** dissolved in CD_3OD in an NMR tube. We have characterized this derivative in the solid state by X-ray crystallography and in solution by ^{13}C NMR spectroscopy (δ = 208.5 and 220.1), thereby demonstrating that it is identical to the methoxide-bridged dimer we reported previously.[23] Presumably, this complex results from pro-

Table 7. Observed first-order rate constants for the CO exchange kinetics in complexes **1**−**4** as a function of temperature

Complex[a]	Temp [°C]	k [s^{-1}] × 10^4
1[b]	35.0	2.750
	40.0	4.617
	45.0	12.97
	50.0	22.35
	57.0	53.13
2[c]	20.0	0.1167
	30.0	0.5000
	40.0	1.567
	50.0	4.733
3[c]	5.0	0.0833
	15.0	0.4500
	30.0	2.600
	40.0	6.133
4[c]	20.0	0.119
	35.0	0.497
	41.3	0.987
	45.0	1.033
	50.0	1.991

[a] Kinetic data on all complexes were obtained as Et_4N^+ salts to avoid significant ion-pairing effects (M. W. Payne, D. L. Leussing, S. G. Shore, *Organometallics* **1991**, *10*, 574). − [b] In THF. − [c] In CH_3CN.

tonation of the dihydrouracilate ligand by methanol to initially afford the $W(CO)_5OMe^-$ anion. This methoxide derivative has been shown to readily undergo CO dissociation and aggregation to the anions $[W(CO)_4(OMe)]_2^{2-}$ and $[W_2(CO)_6(OMe)_3]^{3-}$, or $[W(CO)_3OMe]_4^{4-}$.[23]

The CO lability in complexes **1**−**5** was examined by monitoring CO exchange (Equation 1) using in situ spectroscopy in the ν(CO) region. The decrease in absorbance of the highest frequency ν(CO) band was measured as a function of time with an IR probe inserted directly into an acetonitrile solution of the respective complex maintained at constant temperature with a thermostated water bath. The reactions were performed in the presence of a large excess of ^{13}CO in order to avoid having to consider the reverse process. Table 7 compiles the first-order rate constants for the CO exchange for the various complexes as a function of temperature. Table 8 lists the derived activation parameters for these processes obtained from the data in Table 7 and Figure 8, along with the corresponding values for the $W(CO)_5(uracilate)^-$ anion previously reported.

$$W(CO)_5(uracilate)^- + n^{13}CO \underset{k_2}{\overset{k_1}{\rightleftharpoons}} W(CO)_{5-n}(^{13}CO)_n(uracilate)^- + nCO \quad (1)$$

As is evident from the Eyring plots in Figure 8 for ^{13}CO exchange in complex **1**−**3** and the parent uracilate derivative, there are two distinct regions, one for the N1-bound complexes (**2** and the parent uracilate) and one for the N3-bound derivatives (**1** and **3**). The two complexes bound through the deprotonated N3 center are slightly more reactive towards CO exchange than the two complexes ligated by way of the deprontonated N1 group. Furthermore, within each grouping the presence of an electron-donating methyl substituent in the pyrimidine ring results in a somewhat enhanced rate (factor of 2−3) of CO lability. In other words, this facile CO exchange is attributed to π-donation of electron density from the deprotonated N1 or N3 atoms of the uracilate ligands, thereby stabilizing the developing 5-coordinate metal intermediate. Previously, we have demonstrated for the uracilate derivative that it is the *cis*-carbonyl ligands that are selectively exchanged. Nevertheless, these pyrimidine ligands bound through their endocyclic ni-

Table 8. Activation parameters for CO exchange reactions

Complex[a]	$\Delta H^‡$ [kJ/mol]	$\Delta S^‡$ [J/mol K]	k [s^{-1}][b]
$[W(CO)_5$(dihydrouracilate)$]^-$ (**1**)	114.4 ± 6	57.3 ± 18.8[c]	$5.83\cdot10^{-5}$
$[W(CO)_5$(5-methyluracilate)$]^-$ (**2**)	94.0 ± 2.8	−18.4 ± 9.0[d]	$2.41\cdot10^{-5}$
$[W(CO)_5$(6-methyluracilate)$]^-$ (**3**)	86.0 ± 5.9	−31.0 ± 20.0[d]	$13.3\cdot10^{-5}$
$[W(CO)_5$(uracilate)$]^-$	106.9 ± 4.3	16.3 ± 13.7[d] [e]	$0.86\cdot10^{-5}$

[a] As Et_4N^+ salt. − [b] Computed at 25.0 °C. − [c] In THF. − [d] In CH_3CN. − [e] Ref.[15]

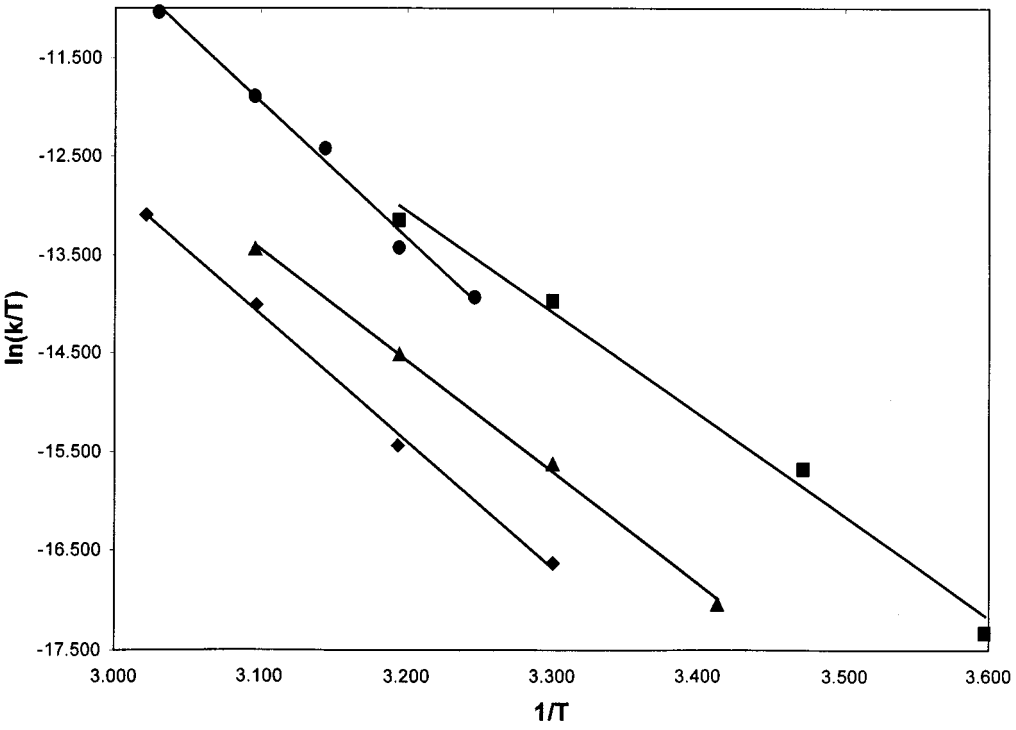

Figure 8. Eyring plots for the first-order CO exchange process involving the $W(CO)_5L^-$ anions and ^{13}CO [L = dihydrouracilate (◆), 6-methyluracilate (●), 5-methyluracilate (▲), and uracilate (■)]

trogen atoms are *considerably less* CO-labilizing than the good π-donating phenolate ligands,[23] and *slightly less* CO-labilizing than the Cl^- ion or the exocyclic sulfur donors in thiouracilate derivatives.[16,23]

The rate constant for CO exchange ($1.88 \cdot 10^{-5}$ s^{-1} at 25 °C) in complex **4**, the closely related methylorotate derivative, is similar to those determined for the other pyrimidine complexes examined herein. The corresponding activation parameters, $\Delta H^{\neq} = 69.6 \pm 3.6$ kJ/mol and $\Delta S^{\neq} = -101.8 \pm 11.6$ J/molK, were derived from the temperature-dependent rate constant data. On the other hand, attempts to determine the kinetic parameters for intermolecular CO exchange in the carboxylate-bound derivative, $[Et_4N][W(CO)_5(N,N\text{-dimethylorotate})]$ (**5**), lead to extensive ligand loss with the formation of ^{13}CO-labeled $W(CO)_6$. Concomitantly, when the substitution reaction was carried out with $P(OEt)_3$ as an incoming ligand the principal product was the neutral complex $W(CO)_5P(OEt)_3$, resulting from displacement of the carboxylate ligand.

Conclusion

Stable tetraethylammonium salts of pentacarbonyltungsten anions of pyrimidine bases have been synthesized from the reactions of $W(CO)_5$(solvent), where solvent = THF or MeOH, with the deprotonated monoanion of the corresponding uracil or orotic acid derivative. Crystal structures of $[Et_4N][W(CO)_5$(dihydrouracilate)] (**1**) and $[Et_4N][W(CO)_5$(6-methyluracilate)] (**3**) reveal that the uracilate ligands are bonded to the tungsten center through the deprotonated N3 atom, whereas $[Et_4N][W(CO)_5$(5-methyluracilate)] (**2**) is bound to the metal fragment by the deprotonated N1 nitrogen atom of the ring. This disparity in binding mode appears to be dictated by steric considerations. In the absence of steric hindrance preferential binding at the N1 position is anticipated.

This difference in metal-binding sites is evident as well, by both IR and ^{13}C NMR spectroscopy. The ν(CO) and $\nu(CO_2)$ vibrational modes of complexes **1** and **3** are quite similar and occur at lower frequencies than the corresponding parameters of complex **2**. This is indicative of a less electron-donating nitrogen center in the latter derivative. This conclusion is also consistent with the more downfield positions of the ^{13}C resonances for the carbonyl ligands in complexes **1** and **3**.

Concomitantly the rates of CO dissociation in the complexes ligated through the deprotonated N3 center (complexes **1** and **3**), are slightly more facile than the corresponding rate in the N1 ligated derivative (complex **2**). This facile CO exchange with labeled ^{13}CO, which is comparable to that seen in the $W(CO)_5Cl^-$ anion but less than that observed in the alkoxide or aryloxide analogs, is attributed to π-donation of electron density from the nitrogen atom of the pyrimidine bases to the tungsten center in the transition state as the CO bond is broken.

Experimental Section

Methods and Materials: All manipulations were performed in a double manifold Schlenk vacuum line under argon or in an argon-filled glovebox. Solvents were freshly distilled under nitrogen from sodium/benzophenone ketyl (tetrahydrofuran, hexane, diethyl ether), magnesium iodide (methanol), or phosphorous pentoxide followed by calcium hydride (acetonitrile). − Photolysis experiments were performed using a mercury arc 450-W UV immersion lamp purchased from Ace Glass Co. − Routine IR spectra were recorded with a Matteson 6022 spectrometer with DTGS and MCT detectors, using a 0.10-mm CaF_2 cell. − Kinetic measurements were monitored with an ASI REACT IR™ 1000 system equipped with an MCT detector and 30 bounce SiCOMP™ in situ probe. − ^{13}C NMR spectra were obtained with a Varian Unity XL-300 spectrometer. − ^{13}CO was purchased from Cambridge Isotopes and used as received. $W(CO)_6$ was purchased from Fluka, and used without further purification. Dihydrouracil, 6-methyluracil, 5-methyluracil, and orotic acid methyl ester were purchased from Aldrich Chemical and used as received. 1,3-dimethylorotic acid was synthesized according to a previously published procedure.[24] − Microanalyses were performed by Canadian Microanalytical Service, Ltd., Delta, B.C.

Synthesis of $[NEt_4][W(CO)_5$(dihydrourcilate)] (1): In a typical synthesis dihydrouracil (0.163 g, 1.43 mmol) was placed in a Schlenk flask with a 25% w/w Et_4NOH solution in methanol (0.85 g, 1.44 mmol), along with 10 mL of THF. This solution was stirred for 45 min and concentrated for about 12 h to provide a white solid. $W(CO)_5THF$ was prepared by photolysis of $W(CO)_6$ (0.50 g, 1.44 mmol) in 60 mL of THF for 45 min. This yellow solution was then transferred to the $[Et_4N]$[diydrouracilate] and 1.5 mL methanol was added to dissolve the salt. The solution turned dark orange red on addition of the methanol. The solution was stirred for 10 min and concentrated to dryness leaving an orange powder. This powder was dissolved in CH_3CN and filtered through Celite leaving a clear orange solution, which was washed with 2 × 20 mL of hexane to remove excess $W(CO)_6$, and a white solid (unchanged $[Et_4N]$[diydrouracilate]). The product was precipitated with diethyl ether and vacuum-dried yielding 0.61 g (75% yield) of an analytically pure orange powder. − $C_{17}H_{25}O_7N_3W$ (567.3): calcd. C 36.00, H 4.44, N 7.41; found C 35.22, H 4.48, N 7.38. − IR (CH_3CN): $\tilde{\nu}$ = 2058 (w), 1911 (s), 1838 (m) cm^{-1}. − ^{13}C NMR (CD_3CN): δ = 202.3 (4 *cis*-CO), 208.0 (*trans*-CO). − Orange block crystals of **1** were obtained by slow diffusion of hexane into a THF solution of $[Et_4N][W(CO)_5(C_4H_5N_2O_2)]$ at 0° C.

Synthesis of $[NEt_4][W(CO)_5$(5-methyluracilate)] (2): In a typical synthesis 5-methyluracil (thymine) (0.179 g, 1.42 mmol) was placed in a Schlenk flask with tetraethylammonium hydroxide (25% w/w in methanol) (0.842 g, 1.43 mmol) and 10 mL of methanol. This solution was stirred for 1 h and vacuum-dried for about 12 h, yielding a white solid. $W(CO)_5THF$ (1.44 mmol), generated as in **1**, was added to this white solid, and 3 mL of methanol was also added to aid in the solubility of the salt. This yellow solution was stirred for 1 h and concentrated to dryness. The resulting yellow/brown solid was redissolved in THF and filtered through Celite leaving a yellow solution and a brown solid. The remaining yellow solution was layered with hexane and 0.49 g (57% yield) of an analytically pure bright yellow powder was obtained. − $C_{18}H_{25}O_7N_3W$ (579.3): calcd. C 37.32, H 4.35, N 7.25; found C 37.39, H 4.38, N 7.19. − IR (CH_3CN): $\tilde{\nu}$ = 2065 (w), 1915 (s), 1855(m) cm^{-1}. − ^{13}C NMR (CD_3CN): δ = 200.7 (4 *cis*-COs), 205.8 (*trans*-CO). − Yellow crystals of **2** were obtained by slow diffusion of hexane into a THF solution of **2** at room temperature over 4 d.

Synthesis of [NEt$_4$][W(CO)$_5$(6-methyluracilate)] (3): The synthesis of **3** was carried out in a manner analogous to that of **2**. 6-methyluracil (0.181 g, 1.44 mmol) was placed in a Schlenk flask with 1 equiv. of tetraethylammonimum hydroxide (25% w/w in methanol), and 10 mL of methanol. This solution was stirred for 2 h and vacuum dried for about 12 h, yielding a white solid. W(CO)$_5$THF (1.44 mmol), generated photochemically, was added to this and 2 mL of methanol was added to aid in its solubility. The resulting cloudy orange solution was filtered through Celite, leaving a clear orange solution. This solution was layered with hexane yielding 0.58 g (66% yield) of an analytically pure yellow powder. − $C_{18}H_{25}O_7N_3W$ (579.3): calcd. C 37.32, H 4.35, N 7.25; found C 37.39, H 4.35, N 7.25. − IR (CH_3CN): $\tilde{\nu}$ = 2059 (w), 1912 (s), 1840 (m) cm^{-1}. − ^{13}C NMR (CD_3CN): δ = 202.0 (4 *cis*-CO), 204.8 (*trans*-CO) cm^{-1}. − Yellow diffraction-quality crystals of **3** were grown by slow diffusion of hexane into a THF solution of **3** at room temperature over 3 d.

Synthesis of [Et$_4$N][W(CO)$_5$(methylorotate)] (4): In a typical synthesis a Schlenk flask was charged with the methyl ester of orotic acid (0.242 g, 1.44 mmol), slurried in 10 mL of THF and deprotonated with a 25% w/w Et$_4$NOH solution in methanol (0.85 g, 1.44 mmol). This solution was stirred for 30 min and the solvent was removed under vacuum, leaving a pale yellow solid. W(CO)$_5$THF was prepared photochemically, starting with W(CO)$_6$ (0.50 g, 1.44 mmol) in 60 mL of THF. This was photolyzed for 45 min. The resulting yellow solution was transferred via a cannula into the flask containing the deprotonated ester. The resulting solution changed color from yellow to a dark yellow-brown. The solution was stirred for 45 min and then concentrated to dryness overnight. The resulting solid was dissolved in CH_3CN and filtered through Celite affording a clear brownish-yellow solution which was washed with hexane to remove any residual W(CO)$_6$. The product was obtained in < 80% yield by the removal of solvent under reduced pressure to give a sticky brown solid. − $C_{19}H_{25}N_3O_9W$ (623.2712): calcd. C 36.61, H 4.04, N 6.74; found C 35.72, H 3.94, N 6.88. − IR (CH_3CN): $\tilde{\nu}$ = 2060 (w), 1914 (s), 1846 (m) cm^{-1}.

Synthesis of [Et$_4$N][W(CO)$_5$(*N*,*N*-dimethylorotate)] (5): A Schlenk flask was charged with *N*,*N*-dimethylorotic acid (0.261 g, 1.44 mmol), slurried in 10 mL of THF and deprotonated with a 25% w/w Et$_4$NOH solution in methanol (0.85 g, 1.44 mmol). This solution was stirred for 30 min and the solvent was removed under vacuum, leaving a white solid. W(CO)$_5$THF was prepared photochemically, starting with W(CO)$_6$ (0.50 g, 1.44 mmol) in 60 mL of THF. This was photolyzed for 45 min. The resulting yellow solution was transferred via a cannula into the flask containing the deprotonated acid. The resulting solution changed color from yellow to a dark orange-yellow. The solution was stirred for 45 min and then concentrated to dryness overnight. The sticky solid was dissolved in CH_3CN and filtered through Celite affording a clear brownish-orange solution which was washed with hexane to remove any residual W(CO)$_6$. The product was obtained in < 80% yield by the removal of solvent under reduced pressure to give a brown-orange solid. − $C_{20}H_{27}N_3O_9W$ (637.3): calcd. C 37.69, H 4.27, N 6.59; found C 37.65, H 4.56, N 6.62. − IR (CH_3CN): $\tilde{\nu}$ = 2067 (w), 1920 (s), 1853 (m) cm^{-1}.

Reaction of 1 with Methanol: Approximately 0.05 g of **1** was placed in an NMR tube with 1 mL of CD_3OD. The orange solution was then placed under ^{13}CO and inserted into an NMR probe. On removal of the tube from the NMR spectrometer, red block crystals of [Et$_4$N]$_2$[W(CO)$_4$(OMe)]$_2$ (**6**) were found. − ^{13}C NMR (CD_3OD): δ = 208.5 (4 *cis*-CO), 220.1 (4 *trans*-CO).

X-ray Crystallography

[Et$_4$N][W(CO)$_5$(dihydrouracilate)] (1): Crystal data and details of data collection are given in Table 9. An orange block of **1** was mounted on a glass fiber with epoxy cement, at room temperature. Preliminary examination and data collection were performed with a Rigaku AFC5R X-ray diffractometer (Cu-K_α, λ = 1.54178 Å radiation) for **1**. Cell parameters were calculated from the least-squares fitting of the setting angles for 24 reflections; ω scans for several intense reflections indicated acceptable crystal quality. Data were collected for 7.62° ≤ 2θ ≤ 120.12°. Three control reflections, collected every 97 reflections, showed no significant trends. Background measurements by stationary-crystal and stationary-counter techniques were taken at the beginning and end of each scan for half of the total scan time. Lorentz and polarization corrections were applied to 3873 reflections for **1**. A semiempirical absorption correction was applied to **1**. A total of 3873 unique reflections with $|I| \geq 2.0\sigma(I)$ were used in further calculations. The structure of **1** was solved by direct methods (SHELXS program package, Sheldrick, **1993**). Full-matrix least-squares anisotropic refinement for all non-hydrogen atoms yielded R = 0.0598, R_w = 0.0634, and S = 1.085 for **1**. Hydrogen atoms were placed in idealized positions with

Table 9. Crystallographic data for complexes **1**−**3** and **6**

	1	**2**	**3**	**6**
Empirical formula	$C_{21}H_{35}N_3O_8W$	$C_{20}H_{30}N_3O_{7.5}W$	$C_{18}H_{25}N_3O_7W$	$C_{19.5}H_{34.5}N_{1.5}O_{7.5}W_{1.5}$
Molecular mass	641.37	614.30	579.26	685.76
Space group	$P\bar{1}$	$C2/c$	$P\bar{1}$	$P\bar{1}$
V [Å^3]	1301.5(5)	4865(8)	1108.1(2)	2450.6(8)
Z	2	8	2	4
$d_{calcd.}$ [g/cm^3]	1.637	1.677	1.736	1.859
a [Å]	10.994(2)	19.76(3)	9.8884(13)	10.216(2)
b [Å]	14.336(3)	21.014(8)	10.4293(12)	11.680(2)
c [Å]	10.922(2)	12.485(11)	11.5381(12)	21.247(4)
α [°]	112.12(3)	−	78.120(9)	97.49(3)
β [°]	110.88(3)	110.18(10)	75.314(10)	95.29(3)
γ [°]	106.69(3)	−	77.158(10)	100.88(3)
T [K]	298(2)	163(2)	173(2)	173(2)
μ(Mo-K$_\alpha$) [mm^{-1}]	8.630	9.195	5.254	7.087
Wavelength [Å]	1.541 78	1.541 78	0.710 73	0.710 73
R_F[a] (%)	5.98	6.65	2.79	4.73
R_{wF} [b] (%)	6.34	14.66	7.04	7.06

[a] $R_F = \Sigma|F_o - F_c|/\Sigma F_o$. − [b] $R_{wF} = \{[\Sigma w(F_o^2 - F_c^2)^2]/(\Sigma wF_o^2)\}^{1/2}$.

the isotropic thermal parameters fixed at 0.08. Neutral-atom scattering factors and anomalous scattering correction terms were taken from the *International Tables for X-ray Crystallography.* Crystallographic data (excluding structure factors) for the structure(s) reported in this paper have been deposited with the Cambridge Crystallographic Data Centre as supplementary publication no. CCDC-148932 (**1**), -148933 (**3**), -148934 (**6**), and -148935 (**2**). Copies of the data can be obtained free of charge on application to CCDC, 12 Union road, Cambridge CB2 1EZ, UK [Fax: (internat.) + 44-1223/336-033; E-mail: deposit@ccdc.cam.ac.uk].

$[Et_4N][W(CO)_5(L)]$ [L = 5-Methyluracilate (2), 6-Methyluracilate (3)]: Crystal data and details of data collection are given in Table 9. A yellow needle of **2** and a yellow block of **3** were mounted on a glass fiber with epoxy cement at room temperature, and cooled in a cold stream of liquid nitrogen. Preliminary examination and data collection were performed with a Rigaku AFC5R X-ray diffractometer (Cu-K_α, λ = 1.54178 Å radiation) for **2**, and a Siemens P4 X-ray diffractometer (Mo-K_α, λ = 0.71073 Å radiation) for **3**. Data collection and parameters are identical to those described for complex **1**. Data were collected for $6.36° \leq 2\theta \leq 100.00°$ for **2** and $4.06° \leq 2\theta \leq 50.00°$ for **3**. Lorentz and polarization corrections were applied to 2437 reflections for **2** and 3887 reflections for **3**. A total of 2437 unique reflections for **2** and 3886 unique reflections for **3** were used in further calculations. Anisotropic refinement for all non-hydrogen atoms yielded $R = 0.0665$, $R_w = 0.1466$, and $S = 0.920$ for **2**, and $R = 0.0274$, $R_w = 0.0704$, and $S = 0.786$ for **3**.

$[Et_4N]_2[W_2(CO)_8(OMe)_2]$ (6): Crystal data and details of data collection are given in Table 9. A red block of **6** was mounted on a glass fiber with epoxy cement at room temperature, and cooled in a cold stream of liquid nitrogen. Preliminary examination and data collection were performed with a Siemens P4 X-ray diffractometer (Mo-K_α, λ = 0.710 73 Å radiation). Data collection and parameters are identical to that described for complex **1**. Data were collected for $4.08° \leq 2\theta \leq 50.00°$ for **6**. Lorentz and polarization corrections were applied to 8614 reflections. A total of 8614 unique reflections were used in further calculations. Anisotropic refinement for all non-hydrogen atoms yielded $R = 0.0473$, $R_w = 0.0706$, and $S = 1.006$.

Kinetic Measurements: The rates of ^{13}CO exchange in complexes **1**−**5** were determined at a variety of temperatures; ^{13}CO was placed over the solution of 0.1 g of the complex in 15 mL of THF or CH_3CN, which was situated in a thermostated temperature bath. The solutions were magnetically stirred and placed in a temperature bath at a variety of temperatures for **1** (35.0, 40.0, 45.0, 50.0, 57.0 °C), **2** (20.0, 30.0, 40.0, 50.0 °C), **3** (5.0, 15.0, 30.0, 40.0 °C), **4** (20, 35, 41, 45, 50 °C), and **5** (30, 40, 50 °C). The kinetics were monitored using ASI ReactIR in situ IR probe, by following the decrease in absorbance of the highest frequency A_1 band in the ν(CO) region of the IR spectrum as a function of time.

Acknowledgments

Financial support from the National Science Foundation (CHE99-10342 and CHE98-07975 for the purchase of X-ray equipment) and the Robert A. Welch Foundation is greatly appreciated.

[1] M. Goodgame, D. A. Jakubovic, *Coord. Chem. Rev.* **1987**, *79*, 97.
[2] I. Mutikainen, *Ann. Acad. Sci. Fenn, Ser. A. II. Chem.* **1988**, 217, and references therein.
[3] J. R. Lusty (Ed.), *CRC Handbook of Nucleobase Complexes: Transition Metal Complexes of Naturally Occurring Nucleobases and Their Derivatives*; CRC Press, Boca Raton, FL, **1990**, vol. 1, pp. 9−99.
[4] M. J. Bloemink, J. Reedijk, in: *Interaction of Metal Ions with Nucleotides, Nucleic Acids and Their Derivatives* (Eds. A. Sigel, H. Sigel), Marcel Dekker, New York, **1996**, pp. 641−685.
[5] D. M. Huryn, M. Okabe, *Chem. Rev.* **1992**, *92*, 1745−1768.
[6] E. DeClercq, *J. Med. Chem.* **1995**, *38*, 2491−2517.
[7] M. Shionoya, E. Kimura, M. Shiro, *J. Am. Chem. Soc.* **1993**, *115*, 6730−6737.
[8] M. Shionoya, T. Ikeda, E. Kimura, M. Shiro, *J. Am. Chem. Soc.* **1994**, *116*, 3848−3859.
[9] S. Aoki, Y. Honda, E. Kimura, *J. Am. Chem. Soc.* **1998**, *120*, 10018−10026.
[10] S. Aoki, C. Sugimura, E. Kimura, *J. Am. Chem. Soc.* **1998**, *120*, 10094−10102.
[11] P. D. Cookson, E. R. T. Tiekink, M. W. Whitehouse, *Aust. J. Chem.* **1994**, *47*, 577.
[12] E. R. T. Tiekink, P. D. Cookson, B. M. Linahan, L. K. Webster, *Metal Based Drugs* **1994**, 299.
[13] W. Beck, N. Kottmair, *Chem. Ber.* **1976**, *109*, 970.
[14] N. Kottmair, W. Beck, *Inorg. Chim. Acta* **1979**, *34*, 134−144.
[15] D. J. Darensbourg, J. D. Draper, D. L. Larkins, B. J Frost, J. H. Reibenspies, *Inorg. Chem.* **1998**, *37*, 2538.
[16] D. J. Darensbourg, B. J. Frost, A. Derecskei-Kovacs, J. H. Reibenspies, *Inorg. Chem.* **1999**, *38*, 4715.
[17] M. Ruf, K Weis, H. Vahrenkamp, *Inorg. Chem.* **1997**, *36*, 2130.
[18] G. W. Hunt, E. A. H. Griffith, E. L. Amma, *Inorg. Chem.* **1976**, *15*, 2993−2997.
[19] D. J. Darensbourg, J. A. Joyce, C. J. Bischoff, J. H. Reibenspies, *Inorg. Chem.* **1991**, *30*, 1137−1142.
[20] D. J. Darensbourg, E. V. Atnip, K. K. Klausmeyer, J. H. Reibenspies, *Inorg. Chem.* **1994**, *33*, 5230−5237.
[21] C. Moralejo, C. H. Langford, P. H. Bird, *Can. J. Chem.* **1991**, *69*, 2033.
[22] [22a] L. Tutt, J. I. Zink, *J. Am. Chem. Soc.* **1986**, *108*, 5830. − [22b] U. Klement, *Z. Kristallogr.* **1993**, *208*, 111.
[23] D. J. Darensbourg, K. K. Klausmeyer, J. D. Draper, J. A. Chojnacki, J. H. Reibenspies, *Inorg. Chim. Acta* **1998**, *270*, 405−413.
[24] P. Beak, B. Siegel, *J. Am. Chem. Soc.* **1976**, *98*, 3601.

Received April 7, 2000
[I00137]